USING DYNAMIC IN VIVO KINEMATICS FOR SUBJECT-SPECIFIC

CALIBRATION OF KNEE LIGAMENT PARAMETERS

by

Stephen Nelson

A thesis

submitted in partial fulfillment

of the requirements for the degree of

Master of Science in Mechanical Engineering

Boise State University

December 2021

BOISE STATE UNIVERSITY GRADUATE COLLEGE

DEFENSE COMMITTEE AND FINAL READING APPROVALS

of the thesis submitted by

Stephen Nelson

Thesis Title: Using Dynamic in Vivo Kinematics for Subject-Specific Calibration of Knee Ligament Parameters

Date of Final Oral Examination: 27 September 2021

The following individuals read and discussed the thesis submitted by student Stephen Nelson, and they evaluated the student's presentation and response to questions during the final oral examination. They found that the student passed the final oral examination.

Clare Fitzpatrick, Ph.D.   Chair, Supervisory Committee

Mahmood Mamivand, Ph.D.   Member, Supervisory Committee

Gunes Uzer, Ph.D.   Member, Supervisory Committee

The final reading approval of the thesis was granted by Clare Fitzpatrick, Ph.D., Chair of the Supervisory Committee. The thesis was approved by the Graduate College.

DEDICATION

This work is dedicated to my family for their support.

ACKNOWLEDGMENTS

ABSTRACT

In vivo clinical studies are the optimal way to investigate the biomechanical outcomes of new prosthetic devices. This particular style of testing can be difficult and, in certain cases, unethical to perform. The testing of unproven devices, surgical techniques, and materials put patients at risk from unanticipated outcomes in how these devices respond to the in vivo environment and patient-specific loading conditions. Biomechanical computational models were developed to provide validation to new devices prior to clinical testing. Computational models for use in optimizing knee prosthetics frequently include ligament representations, but these representations have inherent uncertainty due to wide intersubject variation across the population and difficulties in defining the subject-specific properties of the ligament. Typically, these parameters are tuned using a trial-and-error approach by experienced personnel or by adapting literature values. However, published values for ligament constants have been shown to vary greatly. Due to these issues, previous studies have recommended the use of a sensitivity analysis to validate input parameters and incorporate uncertainty into finite element (FE) analyses. FE simulations have been widely used in implant development, but this has largely been performed using subjects with a normal body mass index (BMI). Increasing BMI has been shown to negatively impact the outcomes of total knee arthroplasty (TKA) procedures. Better understanding of obesity's impact on joint kinematics will help with design refinement for prosthetics used in obese individuals.

The first objective of this study was to use dynamic, in vivo kinematics to bound subject-specific ligament parameters to a region that will produce physiological forces, thus removing some uncertainty associated with ligament properties. A Monte Carlo simulation was used to find the region of physiological properties for each subject across multiple dynamic activities. The resulting, subject-specific regions were then compared between cohorts of high BMI and normal BMI subjects. Significant differences were found between the bounding areas for these groups. Additionally, there were ligaments that had significant differences when age and gender were considered. This study indicates that there are likely cohort-specific differences in in vivo ligament properties.

The secondary objective was to create a model database of three high BMI subjects as they perform five activities of daily living. Subject-specific, FE simulations were created for the three subjects using kinematics that were derived from experimental data of the subjects completing various exercises. Controllers were developed and tuned to apply the muscle forces, matching profiles generated from the kinematic data. The models correctly reflect the target profiles and are a crucial first step to analyze the outcomes of prosthetic devices in the obese population. Industry partners are currently using this model database to virtually implant prosthetic devices and measure how the resulting kinematics match the natural, non-implanted knee.

TABLE OF CONTENTS

LIST OF TABLES

LIST OF FIGURES

LIST OF ABBREVIATIONS

ACLam	Anteromedial Anterior Cruciate Ligament
ACLpl	Posterolateral Anterior Cruciate Ligament
ALS	Anterolateral Structure
A-P	Anterior-Posterior
BMI	Body Mass Index
CT	Computed Tomography
dMCL	Deep Medial Collateral Ligament
DOF	Degree of Freedom
F-E	Flexion-Extension
FE	Finite Element
GRF	Ground Reaction Forces
HSSR	High-Speed Stereo Radiography
I-E	Interior-Exterior
KSS	Knee Society and Function Score
LCL	Lateral Collateral Ligament
MCLa	Superficial Anterior Medial Collateral Ligament
MCLm	Superficial Medial Medial Collateral Ligament
MCLp	Superficial Posterior Medial Collateral Ligament
M-L	Medial-Lateral
MRI	Magnetic Resonance Imagery

PCAPl	Lateral Posterior Capsule
PCAPm	Medial Posterior Capsule
PCLal	Anterolateral Posterior Cruciate Ligament
PCLpm	Posteromedial Posterior Cruciate Ligament
PF	Patellofemoral
PFL	Popliteofibular Ligament
PI	Proportional-Integral
POL	Posterior Oblique Ligament
RMSE	Root Mean Square Error
S-I	Superior-Inferior
TF	Tibiofemoral
TKA	Total Knee Arthroplasty
V-V	Varus-Valgus

CHAPTER ONE: INTRODUCTION

Background

In vivo clinical studies are the optimal way to investigate biomechanical outcomes of new prosthetic devices. This particular style of testing can be difficult and, in certain cases, unethical to perform with unproven devices. The testing of unproven devices, surgical techniques, and materials put patients at risk from unanticipated outcomes in how these devices respond to the in vivo environment and patient-specific loading conditions. Computational models have shown promise as a means of proving these devices prior to clinical testing (Elias and Cosgarea, 2007). One such computational technique, FE simulation, has been developed for over half a century and has been demonstrated to be a reliable method for performing analyses while avoiding the issues resulting from in vivo trials. Utilization of the FE method in preclinical modeling has displayed effectiveness in providing critical insights into performance characteristics of new implant designs (Shu et al., 2020). Wear patterns and design optimization have been two areas that have benefitted from applying the FE method to analyze new implants (Fitzpatrick et al., 2012; O'Brien et al., 2013). While the FE method is beneficial to implant development, there are important considerations that need to be addressed.

To develop biomechanical computational models that are complex enough to provide useful clinical insight to surgeons and implant designers, physiological, subject-specific representations are required. Subject-specific bony geometry and cartilaginous tissue representations are easily obtained through computed tomography (CT) scans or

magnetic resonance imagery (MRI), respectively. However, soft tissues, such as ligaments and muscles, are not always visible in scans, and even when scans can provide some anatomic information, they do not provide any insight into the mechanical properties of these structures. It is understood that ligaments have a large effect on knee joint kinematics. Therefore, their inclusion is crucial for accurate representation of a subject's knee joint (Galbusera et al., 2014).

In FE simulations, two commonly used methods for modeling ligaments are as one-dimensional spring elements or three-dimensional continuum elements. Spring representations are less computationally expensive while still providing clinically useful results and are, therefore, used in the majority of studies (Naghibi Beidokhti et al., 2017; Weiss et al., 2005). A prior study explored wrapping one-dimensional springs around the tibia to more accurately reflect the medial collateral ligament (MCL) geometry. The study concluded that slight shifts were seen in the anterior-posterior (A-P) positioning and valgus rotations were minimally affected. The minor changes seen were indicative that there is not much benefit for the added complexity of three-dimensional chains of one-dimensional ligaments. This same study showed there are three properties that control how a spring type ligament will behave in a model, the slack length (L_0), linear stiffness (k), and initial location of the attachment sites (Blankevoort et al., 1991). These properties affect the forces generated and therefore, the profile of a ligaments force-displacement curve (**Figure 1**).

$$f = 0 \quad \epsilon < 0 \qquad (1)$$

$$f = \frac{1}{4}k\frac{\epsilon^2}{\epsilon_l} \quad 0 \le \epsilon \le 2\epsilon_l \qquad (2)$$

$$f = k(\epsilon - \epsilon_l) \quad \epsilon > 2\epsilon_l \qquad (3)$$

where,

$$\epsilon = \frac{L - L_0}{L_0}$$

$$\epsilon_l = 0.03$$

Figure 1.   Typical Force-Displacement curve. Region 'A' is the zero-force region - current ligament displacement is below the slack length of the ligament – eq (1). Region 'B' is the non-linear region where the displacement is above the slack length, but all of the ligament fibers are not aligned with the direction of displacement – eq (2). Region 'C' shows the linear region – all fibers are aligned with the displacement – eq (3).

Specific ligament properties fluctuate from subject to subject due to differences in individual biology (Saha and Roychowdhury, 2009). Actual values for the parameters can only be obtained through ex vivo experiments. Typically, the parameters used in an FE study are tuned using a trial-and-error approach by experienced personnel or are adapted from published literature values (Shin et al., 2007). However, published values for

ligament constants have been shown to vary substantially from study to study. Additionally, different combinations of parameters can lead to nearly identical kinematic outputs from a simulation. Due to these issues, previous studies have recommended the use of a sensitivity analysis to validate input parameters and reduce uncertainty in FE simulations (Weiss et al., 2005).

Research Goals

This thesis has two objectives. The first objective is to use dynamic in vivo kinematics to bound subject-specific ligament parameters to a region that will produce physiological forces, thus removing some uncertainty associated with ligament properties. A high and normal BMI cohort, with six subjects in each cohort will be compared. Comparisons of the feasible ligament properties between these two groups will be a first step to further understanding the role increasing BMI plays on the properties of tibiofemoral (TF) ligaments. It is hypothesized that the subjects with high BMIs will have more lax ligaments resulting from the increased loading conditions present as they perform everyday activities. Anecdotal evidence has suggested that the posterior cruciate ligament (PCL) has been compromised in high BMI populations. Through the increased load present in high BMI subjects, it is believed that the PCL experiences higher strain causing degradation of the fibers leading to a lack of recruitment of this ligament. This analysis will be a first step in determining the veracity of this claim.

A secondary objective of this thesis is to use the FE method to develop a model library of three of the high BMI subjects as they complete five activities of daily living. The ligament parameters will be obtained using two methods. Firstly, they will be found

using a manual tuning procedure. Then, they will be selected from the bounds created from the uncertainty study implemented in the first objective. Comparisons of the kinematics resulting from these two methods will allow for further validation of the approach of creating physiological bounds for ligament property sampling. These models will aid in understanding the different loading conditions that exist for individuals within this population and can be used by implant designers in the development of longer-lasting prosthetics for this patient cohort.

CHAPTER TWO: MANUSCRIPT "USING DYNAMIC IN VIVO KINEMATICS FOR

SUBJECT-SPECIFIC CALIBRATION OF KNEE LIGAMENT PARAMETERS"

Introduction

In vivo clinical studies are the optimal way to investigate biomechanical

outcomes of new prosthetic devices. This particular style of testing can be difficult and,

in certain cases, unethical to perform with unproven devices. The testing of unproven

devices, surgical techniques, and materials put patients at risk from unanticipated

outcomes in how these devices respond to the in vivo environment and patient-specific

loading conditions. Computational models have shown promise as a means of proving

these devices prior to clinical testing (Elias and Cosgarea, 2007). One such computational

technique, FE, has been developed for over half a century and has been demonstrated to

be a reliable method for performing analyses while avoiding the issues resulting from in

vivo trials. Utilization of the FE method in preclinical modeling has displayed

effectiveness in providing critical insights into performance characteristics of new

implant designs (Shu et al., 2020). Wear patterns and design optimization have been two

areas that have benefitted from applying FE to analyze new implants (Fitzpatrick et al.,

2012; O'Brien et al., 2013). While FE is beneficial to implant development, there are

important considerations that need to be addressed.

To develop biomechanical computational models that are complex enough to

provide useful clinical insight to surgeons and implant designers, physiological, subject-

specific representations are required. Subject-specific bony geometry and cartilaginous

tissue representations are easily obtained through computed tomography (CT) scans or magnetic resonance imagery (MRI), respectively. However, soft tissues, such as ligaments and muscles, are not always visible in scans, and even when scans can provide some anatomic information, they do not provide any insight into the mechanical properties of these structures. It is understood that ligaments have a large effect on knee joint kinematics. Therefore, their inclusion is crucial for accurate representation of a subject's knee joint (Galbusera et al., 2014).

In FE, the two commonly used methods for modeling ligaments are as one-dimensional spring elements or three-dimensional continuum elements. The spring representations are less computationally expensive while still providing clinically useful results and are, therefore, used in the majority of studies (Naghibi Beidokhti et al., 2017; Weiss et al., 2005). A prior study explored wrapping one-dimensional springs around the tibia to more accurately reflect the medial collateral ligament (MCL) geometry. The study concluded that slight shifts were seen in the anterior-posterior (A-P) positioning and valgus rotations were minimally affected. The minor changes seen were indicative that there is not much benefit for the added complexity of three-dimensional chains of one-dimensional ligaments. This same study showed there are three properties that control how a spring type ligament will behave in a model, the slack length (L_0), linear stiffness (k), and initial location of the attachment sites (Blankevoort et al., 1991). These properties affect the forces generated and therefore, the profile of a ligaments force-displacement curve (**Figure 1**).

$$f = 0 \quad \epsilon < 0 \qquad\qquad (1)$$

$$f = \frac{1}{4}k\frac{\epsilon^2}{\epsilon_l} \quad 0 \leq \epsilon \leq 2\epsilon_l \qquad (2)$$

$$f = k(\epsilon - \epsilon_l) \quad \epsilon > 2\epsilon_l \qquad (3)$$

where,

$$\epsilon = \frac{L - L_0}{L_0}$$

$$\epsilon_l = 0.03$$

Specific ligament properties fluctuate from subject to subject due to differences in individual biology (Saha and Roychowdhury, 2009). Actual values for the parameters can only be obtained through ex vivo experiments. Typically, the parameters used in an FE study are tuned using a trial-and-error approach by experienced personnel or are adapted from published literature values (Shin et al., 2007). However, published values for ligament constants have been shown to vary substantially from study to study. Additionally, different combinations of parameters can lead to nearly identical kinematic outputs from a simulation. Due to these issues, previous studies have recommended the use of a sensitivity analysis to validate input parameters and reduce uncertainty in FE simulations (Weiss et al., 2005). The objective of this study is to develop a method for using dynamic, in vivo kinematics to bound subject-specific ligament properties used in FE to a region that will produce physiological forces, thus reducing uncertainty associated with these properties.

Methods

Experimental Testing

This study's cohort consisted of six participants with a normal BMI (BMI < 25 kg/m^2) and six high BMI ($\geq$ 25 kg/m^2) participants with an average age of 66 ± 9.1 years for both groups combined. The average BMI for the normal BMI cohort was 21.8 ± 2.4 kg/m^2 and the average for the high BMI group was 32.4 ± 3.9 kg/m^2. There were five

female and seven male participants in the study. All subjects provided informed consent to a protocol approved by the University of Denver Institutional Review Board and underwent unilateral lower extremity CT and MRI scans. High-speed stereo radiography (HSSR) data were captured at the knee joint for each subject performing various activities of daily living – seated knee flexion, lunge, 90° pivot, incline, decline, step up, step down, chair rise, level gait, leg press, and kneeling (**Figure 2**).
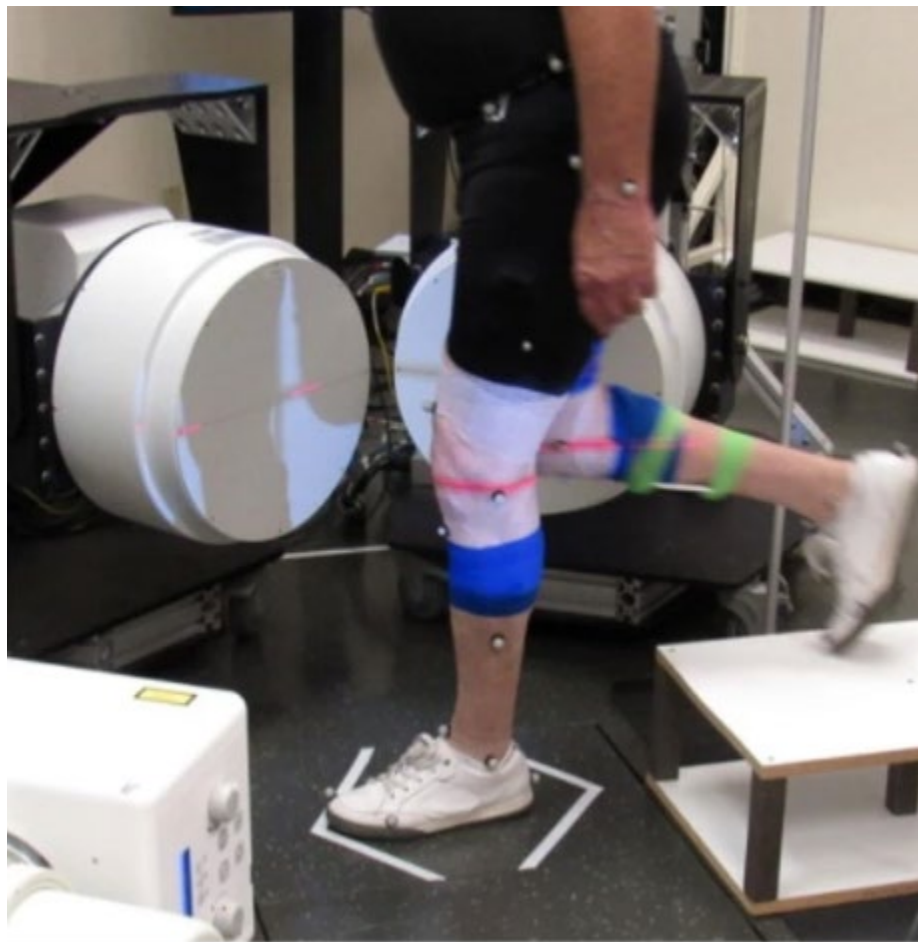
Figure 2.   Experimental data collection setup for the step down activity showing the two radiography sources (HSSR) in the background (Hume et al., 2018).

Additionally, each subject was recorded using retroreflective markers and a ten camera, motion-capture system to describe hip and ankle kinematics. Ground reaction forces (GRF) were obtained by having the participants perform the activities atop a load

cell. TF kinematics were calculated from the HSSR data and described using Grood and Suntay conventions (Grood and Suntay, 1983). This was done by tracking points placed on anatomical landmarks on the tibia, femur, and patella. These points defined coordinate systems that were local to each bone. By calculating the motions of the coordinate systems of the patella and tibia relative to the femur, motions were described in six degrees of freedom (DOF) that are clinically relevant. Hip and ankle kinematics were derived from the motion-capture data.

Kinematic Recalculation

HSSR data has superior joint kinematic accuracy to motion-capture alone, but still contains measurement errors and uncertainty (Hume et al., 2018). These errors have been reported on the order of 0.15mm and 0.41° in translational and rotational DOF, respectively (Ivester et al., 2015). In particular, error and uncertainty in varus-valgus (V-V) and superior-inferior (S-I) DOFs can result in overclosures, wherein one bone partially intersects another bone, or lift-off when the HSSR data are directly used (**Figure 3**). The purpose of the recalculation was to use subject-specific geometry and enforce contact to remove the issues present in the V-V and S-I DOF by leaving them unconstrained to settle naturally in the FE model. The flexion-extension (F-E) and internal-external (I-E) rotations and anterior-posterior (A-P) and medial-lateral (M-L) translations were prescribed.
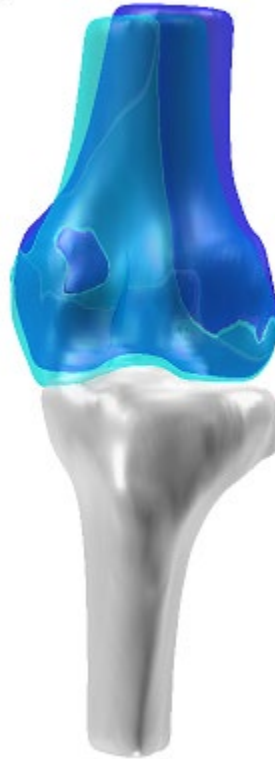
Figure 3. **Comparison of the raw HSSR data (light blue) with the recalculated kinematics (blue) for the same frame of the same activity. Changes present with the V-V angle and the S-I position of the femur.**

A basic FE simulation using Abaqus (Dassault Systèmes, Vélizy-Villacoublay, France) was run to recalculate the TF kinematics to remove these measurement errors. This model only consisted of the femur and tibia bones and cartilage. Contact domains were imposed between the cartilaginous bodies to prevent the overclosures present in the data and a small compressive force was applied to ensure medial and lateral contact throughout the activities. The locations of the bones were tracked throughout the simulation of each activity performed by the subjects. From these relative bony positions, a modified set of kinematics were calculated using the same Grood and Suntay conventions as was used in the HSSR measurements (Grood and Suntay, 1983). The three clinically relevant rotations and translations were used as inputs in the ligament sensitivity study.

In addition to the activities each subject performed, an additional four activities were simulated to help with the validation of results in the ligament simulation. A study by Harris et al. described various rotations and translations that would produce force within a ligament (Harris et al., 2016). These activities were used as one of three tests within the sensitivity study to ensure that the simulated ligament will produce force in a physiological manner. A 4° varus rotation should produce force in the anteromedial anterior cruciate ligament (ACLam), the posterolateral ACL (ACLpl), and the lateral collateral ligament (LCL). A 25° internal rotation was used to validate the anterolateral structure (ALS) and the posterior oblique ligament (POL) results. A 20° external rotation validated the deep medial collateral ligament (dMCL), the superficial anterior MCL (MCLa), the superficial medial MCL (MCLm), the superficial posterior MCL (MCLp), and the popliteofibular ligament (PFL) results, and a 6mm posterior translation was imposed to produce force in the anterolateral posterior cruciate ligament (PCLal) and the posteromedial PCL (PCLpm).

<u>Sensitivity Study</u>

A Monte Carlo simulation was used to find the viable physiological range of ligament properties for each subject's TF joint across the multiple dynamic activities. Previous FE studies have used the ACLam, ACLpl, ALS, LCL, MCLa, MCLm, MCLp, dMCL, POL, the medial and lateral posterior capsule (PCAPm, PCAPl), PCLal, PCLpm, and PFL and so these ligaments were the focus of the analysis (Harris et al., 2016). The initial locations of these ligaments were determined based upon bony prominences for each subject. The ACLam, ACLpl, PCLal, PCLpm, and POL were all represented with two spring elements. The ALS, dMCL, LCL, PCAPl, PCAPm, and PFL all contained

three parallel spring elements, and the superficial MCLa, MCLm, and MCLp each consisted of a single spring element (**Figure 4**).
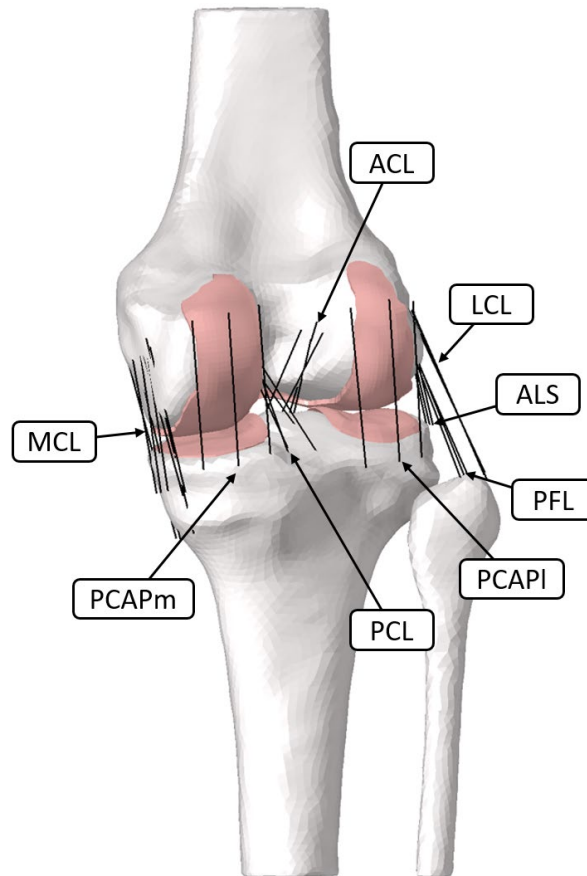
Figure 4. **TF ligament positions for one subject.**

The linear stiffness of the seven TF ligaments were perturbed within ranges centered on values reported in the literature (**Table 1**). The literature value was scaled between 25% and 300% to explore the entire reported range of linear stiffness values. The insertion locations were perturbed ± 3mm in physiological directions – no ligament was permitted to be inserted inside a bone or floating in space far away from the bone. The slack length bounds were determined by scaling the length of the ligament in a full extension pose by 50% - 200% to ensure exploration of all situations where a ligament is either taut or slack at full extension. Using MATLAB (Mathworks, Natick, MA), 100,000

Monte Carlo trials per ligament bundle applied the recalculated, experimentally measured kinematics to all six DOF of the model while the ligament lengths were tracked. Forces generated in each ligament were calculated from the force-displacement curve described by the ligament property parameters. Each ligament parameter was randomly sampled from a uniform distribution of the literature-based ranges in these trials. Failure loads were determined from literature (Butler et al., 1992; Chandrashekar et al., 2006; Ciccone et al., 2006; Harner et al., 1995; Kennedy et al., 1976; LaPrade et al., 2005; Peters et al., 2018; Race and Amis, 1994; Rachmat et al., 2015; Rahnemai-Azar et al., 2016; Robinson et al., 2005; Shin et al., 2007; Woo et al., 1991).

Table 1. **Literature values for linear stiffness and rupture force ([1]Chandrashekar et al., 2006; [3]Ciccone et al., 2006; [6]Harner et al., 1995; [9]Kennedy et al., 1976; [7]LaPrade et al., 2005; [8]Rachmat et al., 2015; [2]Rahnemai-Azar et al., 2016; [4]Robinson et al., 2005; [5]Shin et al., 2007).**

Bundle	Linear Stiffness Range (N/mm)	Rupture Force (N)
ACLam,pl	62.5 - 750[1]	1526[1]
ALS	6.5 - 78[2]	319.7[2]
LCL	20.5 - 246[3]	460[3]
dMCL	10.5 - 126[4]	507[4]
MCLa,m,p	20 - 240[4]	507[4]
POL	14 - 168[4]	507[4]
PCAPl	13.7 - 163.8[5]	500[8]
PCAPm	13.2 - 157.8[5]	500[8]
PCLal	30 - 360[6]	1051[9]
PCLpm	14.3 - 171[6]	1051[9]
PFL	7.2 - 85.8[7]	298.5[7]

Trials which induced ligament forces above 80% of the failure thresholds were classified as non-physiological and discarded. A study on three subjects ACL ligaments showed that failure in the ligament began between 47%-84% of the maximum load. The maximum load in this study was significantly lower than other published results, but due to a lack of published sources on when failure in a ligament begins, the 80% threshold was set (Aggelis et al., 2011). The results were further constrained by removing combinations of parameters that generated less than 25N of force during all activities, as the assumption was that every ligament should be active during at least one of the activities. Finally, the data were constrained using the four validation activities – 4° varus rotation, 25° internal rotation, 20° external rotation, and 6mm posterior translation – by requiring that the ligaments specified should be recruited during these activities. By plotting all of the remaining data points on a single scatter plot, it is possible to create a region to sample ligament parameters that will be within physiological force ranges.

<u>FE Model</u>

The subject-specific models were developed by extracting geometry from the MRI and CT scans using Amira (Thermo Fisher Scientific, Waltham, MA). Three-node triangular surface meshes were made on the bony geometry using HyperMesh (Altair Engineering Inc., Troy, MI) and the cartilage was meshed using a publicly available algorithm to create an eight-node hexahedral continuum mesh (Rodriguez-Vila et al., 2017). This model consisted of femoral, tibial, and patellar bones, corresponding articular cartilage, two patellofemoral (PF) ligaments, and the seven TF ligaments divided into physiological bundles. The bones were defined as rigid bodies and were rigidly attached to the cartilage. The cartilage was also defined as rigid with a pressure-overclosure

relationship defined between the femoral and tibial cartilage and also between the femoral and patellar cartilage (Halloran et al., 2005).

Point-to-point connectors were placed upon estimated lines of action for the biceps femoris long head, biceps femoris short head, lateral and medial gastrocnemius, and the semimembranosus muscles. The quadriceps femoris consisted of multiple lines of action to represent the rectus femoris and the vastus lateralis, medialis, and intermedius. Membrane sections, consisting of 2D elements and springs, were used to represent the various tendons for the quadriceps femoris and attached the muscle lines of action to the patella. Additionally, a membrane section was used to define the patellar tendon connecting the patella to the tibia. To aid in visualizing the results, the head of the femur, the ankle joint, and foot bones were also included in this model (**Figure 5**).
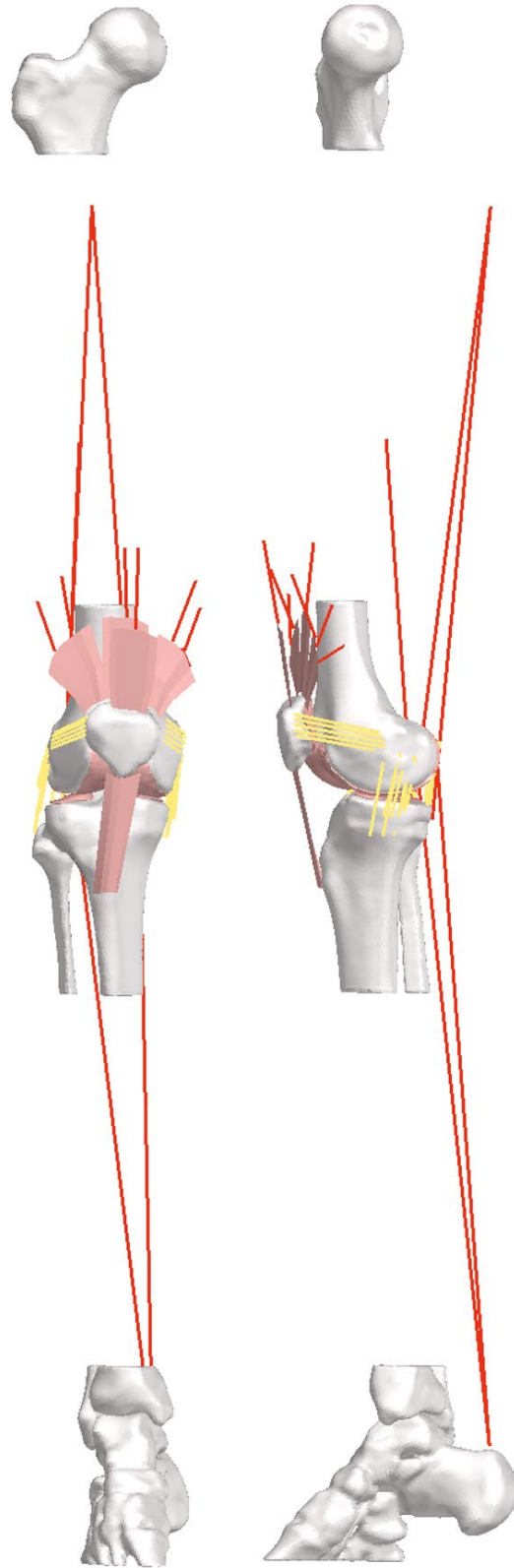
Figure 5. **Frontal and sagittal views of the subject-specific, lower limb model geometry. Ligaments shown in yellow, tendons and cartilage pink, and muscles red.**

<u>Application to Lower Limb Simulations</u>

      The lower limb FE model was run with the ligament parameters sampled from scatter plots of the remaining, physiological points. The hip and ankle kinematics were prescribed from inverse kinematic data generated subsequent to the motion-capture process using the open source software OpenSim (Delp et al., 2007). A FORTRAN subroutine was used to create a proportional-integral (PI) controller at the TF joint to match target F-E profiles that were generated from the HSSR data. The M-L, S-I, and V-V DOF were left free to settle into a natural position driven by the subject-specific geometry. The I-E and A-P DOF were also left free and were tracked to see how the various ligament properties influenced the kinematics for these two DOF. The controller adjusts the current F-E angle by applying force to the quadriceps or hamstring muscles to induce extension or flexion, respectively. The various other muscles in the simulation had forces applied that were determined by a static optimization procedure using the motion-capture data processed in OpenSim. GRF data were applied to the ankle in the appropriate x-, y-, and z-directions.

      Five points were sampled from the scatter plots. The first point was the mean of the scatter plot and then 1.25 times the standard deviation was added/subtracted from the mean to produce four additional points equally spread across the space (**Figure 6**). The 1.25 standard deviation was picked as it will include approximately 80% of the points in the space resulting in a good spread of selected points without containing the boundaries of the plots. The closest plotted point was associated to these five points and the corresponding slack length, linear stiffness, and insertion locations were written to individual files for use in the FE simulation. In order to constrain the number of analyses

to a feasible range, the only ligaments sampled were the MCL and PCL as they play the

largest role in I-E and A-P motions, respectively. A Latin hypercube sample was used to

create 70 combinations of the sampled parameters for 7 of the 14 different ligament

bundles (MCLa, MCLm, MCLp, dMCL, POL, PCLal, and PCLpm). Each of these 70

combinations was run for five different activities performed by one high BMI subject.

The I-E and A-P kinematics were recorded and compared against a baseline set by a

manual tuning of the ligament parameters which has been constrained only by the ranges

reported in literature.
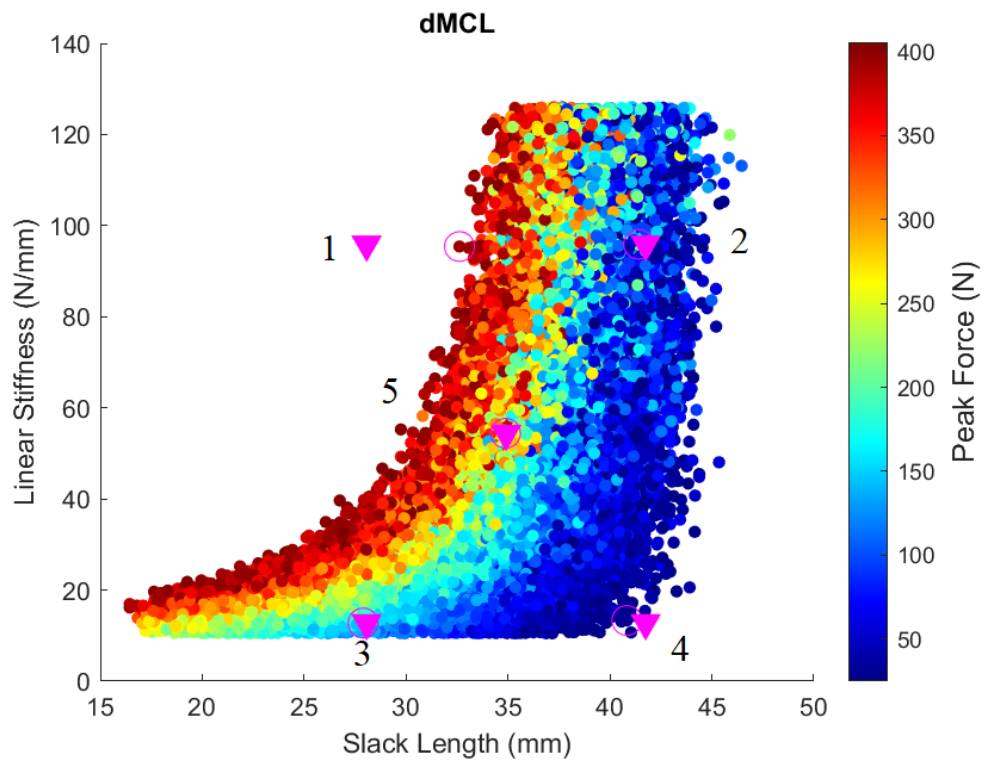
Figure 6. **Five points sampled for the dMCL ligament. Point 5 is the mean and 1-4 are spread by ± 1.25 times the standard deviation. The scatter plot is the remaining points from the sensitivity analysis formed by plotting the slack length (mm) vs linear stiffness (N/mm). The color of the points is based upon the peak force experienced across all of the activities.**

<u>Statistical Analysis</u>

Using MATLAB, one-way ANOVA tests were run with three different cohorts. High and normal BMI, male and female, and elderly and non-elderly (cutoff age of 65 years) were the groups that were compared. Due to a high statistical power from the large number of remaining points from the sensitivity simulation, the effect size was also calculated to determine the magnitude of the difference between the groupings using Cohen's d test. A combination of a significant p-value ($\alpha < 0.05$) and an effect size greater than 0.80 (large) were used as the criteria for determining significant results.

Results

<u>Sensitivity Study</u>

Differences were found when all cohorts were compared – BMI, gender, and age. Six of 14 ligaments studied varied significantly when BMI was compared – ACLam, ACLpl, dMCL, MCLa, MCLm, and MCLp (**Table 2**). It was found that all significant ligaments were slacker for high BMI subjects than the normal BMI subjects (**Figure 7**). The effect size of 2.22 for the ACLpl was the largest effect seen in the study and is highly indicative that a measurable difference exists between the two populations studied for this particular ligament bundle. Four of the five bundles of the MCL also showed substantial variation when comparing the groups based upon BMI with the POL approaching a significant effect, but not to the cutoff of a 0.80 effect size. All of the intergroup differences for the MCL were seen only in the slack length parameter; the linear stiffness did not vary significantly between the BMI groups. However, for the ACLam and ACLpl there were significant differences seen for the linear stiffness parameter. There were very few linear stiffness variations found between all of the cohorts.

Table 2. **ACL and MCL slack lengths and associated effect sizes from the BMI comparison.**

Bundle	Group	Slack Length (mm)	Effect Size
ACLam	High BMI	41.40 ± 4.90	1.76
	Normal BMI	33.13 ± 4.72	
ACLpl	High BMI	32.26 ± 3.63	2.22
	Normal BMI	22.79 ± 4.39	
dMCL	High BMI	34.10 ± 6.10	0.91
	Normal BMI	28.54 ± 6.07	
MCLa	High BMI	56.88 ± 5.85	1.77
	Normal BMI	47.31 ± 5.16	
MCLm	High BMI	50.69 ± 6.80	0.80
	Normal BMI	46.05 ± 4.92	
MCLp	High BMI	48.75 ± 6.63	0.91
	Normal BMI	43.41 ± 5.02	
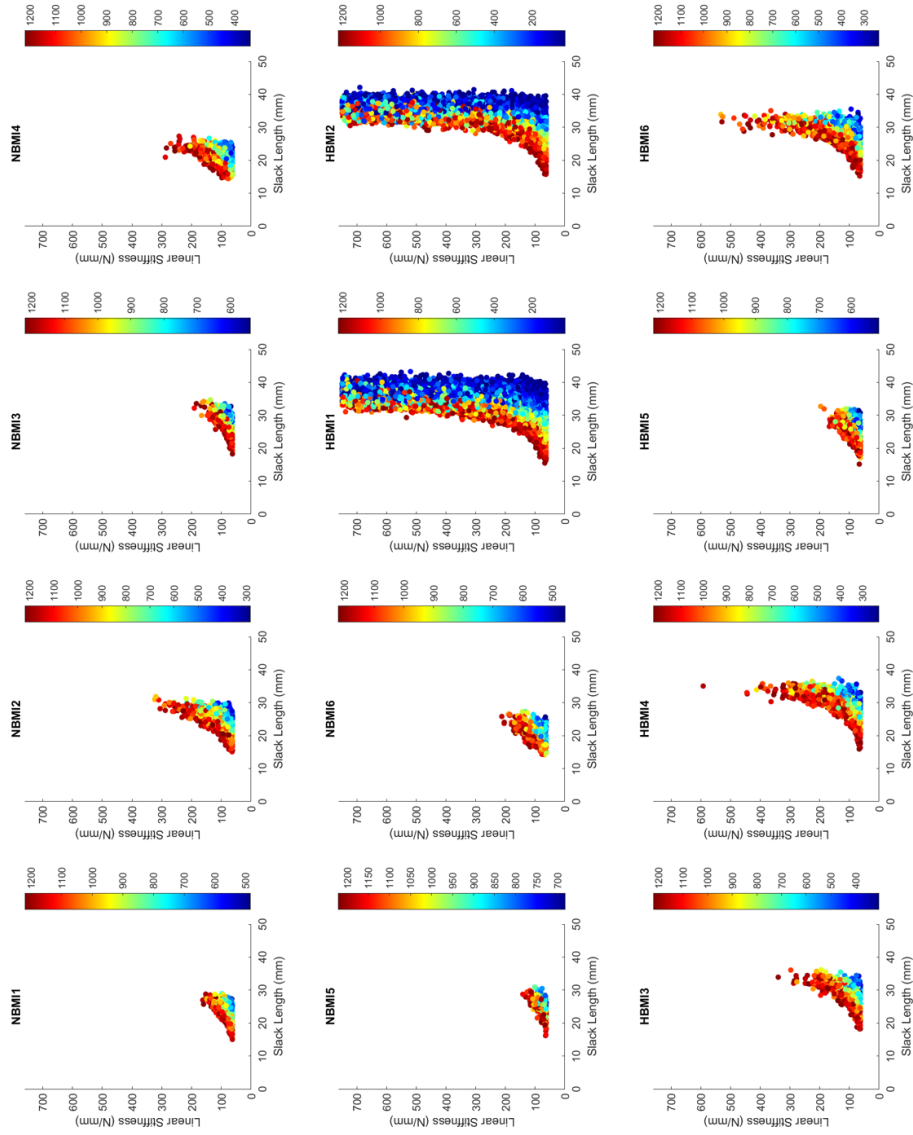
Figure 7. ACLpl resulting scatter plots for all six Normal BMI (NBMI) and all six High BMI (HBMI) subjects in the study. Slack length (mm) vs linear stiffness (N/mm) plots. Color is peak force (N).

Age comparisons had the fewest slack length differences with only the ACLam, ACLpl, MCLa, and PFL producing significant differences when comparing elderly and non-elderly populations (**Table 3**). The differences found in all of these ligaments except for the PFL showed that the elderly population had a lower slack length when compared to the non-elderly population. The largest differences in effect size were seen in the ACLpl and PFL ligaments at 1.39. Similar to the BMI comparison, the ACLam and ACLpl also had significant variation in the linear stiffness paramter.

Table 3.   **Slack length results of the elderly vs. non-elderly comparison.**

Bundle	Group	Slack Length (mm)	Effect Size
ACLam	Elderly	35.52 ± 5.55	1.05
	Non-Elderly	41.05 ± 5.20	
ACLpl	Elderly	25.31 ± 4.79	1.39
	Non-Elderly	31.96 ± 4.78	
MCLa	Elderly	50.09 ± 6.95	0.94
	Non-Elderly	56.08 ± 5.97	
PFL	Elderly	42.46 ± 6.56	1.39
	Non-Elderly	34.20 ± 5.45	

Gender did have an impact on the properties of the ligaments with ALS, LCL, MCLa, MCLm, MCLp, and the PFL showing variation between males and females in the study (**Table 4**). In all of the ligaments with significant variation, males had the larger slack length over females. The only significance found with linear stiffness appeared in both bundles of the ACL when BMI and age were compared. Comparing genders did not bear out the same result. Other ligaments were approaching a large effect size; however, they did not meet the criteria used for inclusion in this study. Most ligaments had

negligible effect sizes for linear stiffness, indicating no intergroup differences for this particular parameter.

Table 4.   Results for slack length when genders were compared.

Bundle	Group	Slack Length (mm)	Effect Size
ALS	Female	24.70 ± 4.54	1.19
	Male	32.12 ± 7.43	
LCL	Female	45.81 ± 4.25	0.97
	Male	50.15 ± 4.98	
MCLa	Female	48.12 ± 5.88	1.67
	Male	57.04 ± 4.96	
MCLm	Female	45.26 ± 5.71	0.99
	Male	50.76 ± 5.45	
MCLp	Female	43.35 ± 5.76	0.82
	Male	48.14 ± 5.87	
PFL	Female	34.36 ± 6.41	0.82
	Male	40.22 ± 7.64	

Application to Lower Limb Simulations

The exploration of the viable, physiological ligament space produced varying results for the I-E and A-P profiles. The goal was to find combinations of ligament parameters that would result in physiological forces while also producing kinematics that most accurately reflect the HSSR data. Four of the five activities (flexion, lunge, 90° pivot, and chair rise) had relatively low root mean square errors (RMSE) as compared to the step down activity, specifically in the A-P profile. For the four activities, the average A-P RMSEs from the 70 simulations were all at or below 6.25mm. Whereas, for the step down activity, the average RMSE was 9.95mm. Therefore, cutoff RMSE values of

9.9mm for the A-P profiles and 10° for the I-E profiles were applied to filter the results. From the 70 initial versions run, a different number of versions remained in the filtered results for each of the five activities. Then, by finding the common ligament parameter combinations between these five filtered activities, plots were created that showed the viable boundaries of the space created from the new ligament properties (**Figure 8**). The intersection of the common versions left 22 ligament combinations that were used to produce these bounding areas.
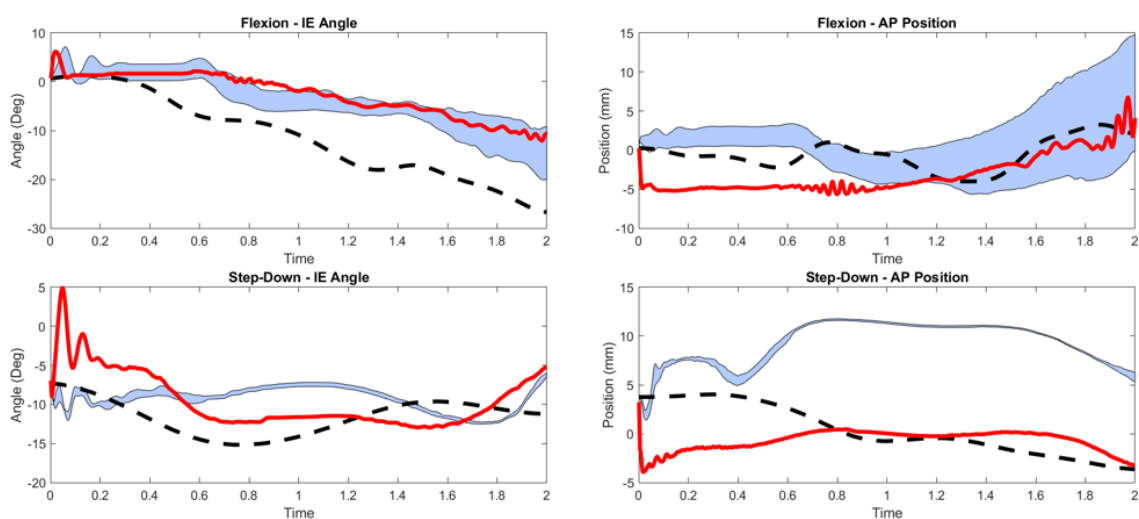
Figure 8.   **I-E and A-P profiles from the boundaries of the exploration study. Flexion and step-down activities shown. The target HSSR profile is shown as a dashed black line, the boundaries from the sampling of the viable ligament space are blue, and results of the manual tuning are plotted in red.**

Discussion

Sensitivity Study

Slack length was more commonly found to be the significant factor when comparing high and normal BMI, which is consistent with the hypothesis that the increased force from increasing BMI will strain a ligament causing the slack length to grow over repeated loading and unloading cycles. The scatter plots of the various

remaining ligament parameters were different in how widely they spanned the sampled parameters. Broadly, the ligaments appeared to be less sensitive to perturbations in linear stiffness with many of the plots of viable ligament properties having linear stiffness values span the sampled space. The one notable exception to this was the ACL which, as previously mentioned, was the singular ligament that significantly differed between high and normal BMI and age groupings. Perturbing the slack length tended to have more substantial impacts on the force generated within the ligament.

As expected, most ligaments appeared to have fairly stratified resulting forces where when slack length was increased, the maximum force generated within the ligament decreased. The ALS appeared the most stratified with clear boundaries as the slack length increases. Conversely, the MCLm and MCLp were fairly random with very low peak forces seen at lower slack lengths and high forces being seen at lower slack lengths (**Figure 9**). Interestingly, the age comparison showed that the elderly subjects tended to have a shorter slack length for both bundles of the ACL. This counterintuitive result is possibly explained by the fact that the normal BMI cohort in this study had an average age of 68.5 ± 9.8 years as compared to the older, high BMI cohort's average age of 63.3 ± 8.38 years. This may be an indication that BMI has a more deleterious effect on ligaments than does aging. When genders were compared, it was always found that males had larger slack lengths than females, and all of these differences appeared in ligaments that are on the lateral or medial sides of the TF joint. A previous study compared the total length of the ALS, ACL, and LCL between genders and found that the ALS and ACL total lengths varied between genders, but the LCL did not (Hohenberger et al., 2019). The

longer slack length in the ALS of males is potentially explained by the longer total

ligament length.
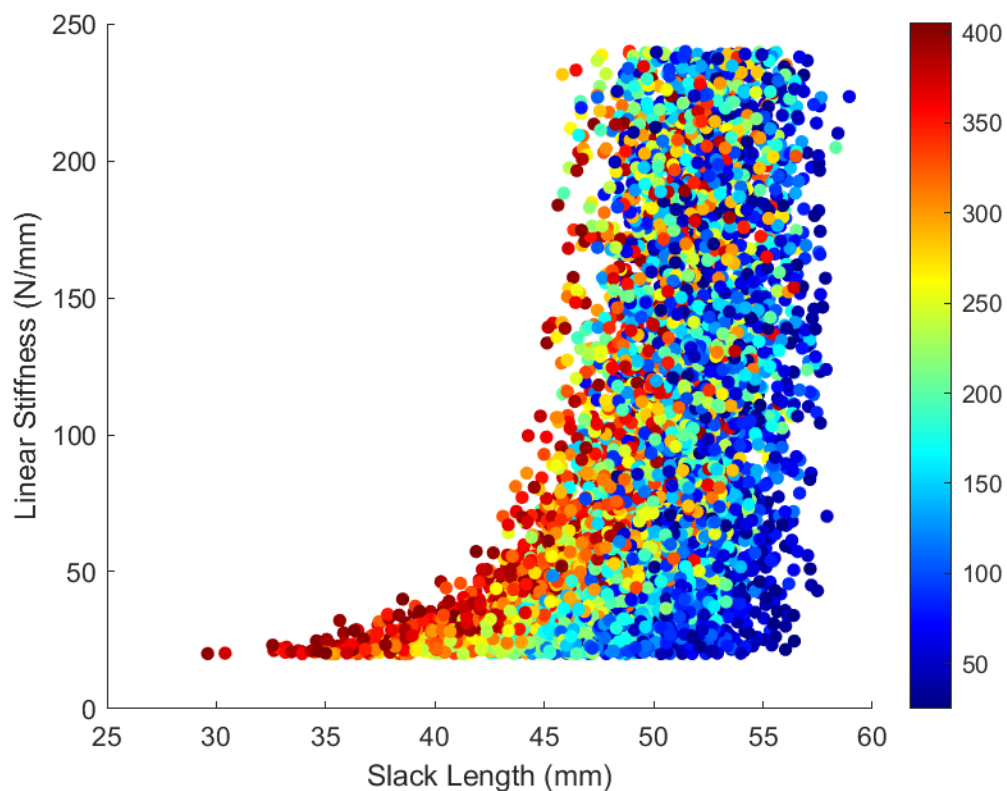
Figure 9. **Sample MCLp plot for HBMI1. High forces can be found at lower slack lengths and low forces seen at shorter slack lengths.**

<u>Application to Lower Limb Simulations</u>

The bounding area from the exploration of these ligament parameters for the A-P

profile on the step down activity had the tightest bounds, seemingly indicating that when

the ligaments are producing physiological forces, the geometry is driving the tibia into a

different position relative to the femur. For all of the other activities, the A-P boundary

appears to vary widely showing that the ligaments play a larger role in those activities.

The I-E boundaries tended to track fairly well with the target data and manual tuning

producing similar results to the sensitivity study. It is worth recognizing that the I-E and

A-P DOF are left unconstrained in these simulations, and in reality, there are other loads from hips, ankles, or other soft tissues, such as adipose tissue, left out of the model that result in the HSSR kinematic targets.

The comparison of the bounding area with the results of the manual tuning is illustrative of the benefits of this study. The A-P plots in all of the activities, except the chair rise, show a large translation from the manual tuning. This translation is driven by a large force that is built up in the ACL, specifically, the ACLpl bundle, from moving the TF joint into the starting position for the activity. The properties settled on in the manual tuning for the ACLpl are outside of the acceptable bounds from the sensitivity study leading to forces that are non-physiological for this ligament bundle. As soon as the tension in that ligament is released by causing an A-P shift in the tibia, the profile matches the trends shown in the boundaries of the exploration study.

Conclusion

Further work is needed in order to measure the sensitivity of the seven untested ligament bundles. Additionally, refinement of the process needs to be considered. A requirement that a ligament only carry 80% of the reported rupture force may ensure that the ligament force in a simulation is physiological, but given simplifications in the FE model, an argument may be made to justify a ligament carrying more force in a simulation than it would realistically.

This study developed a successful method for producing a sampling region for ligament properties that will result in realistic ligament forces in FE simulations. The method used is adaptable for use in any study that has six-DOF kinematics for a knee

joint. This work provides a valuable method for any FE study to more easily calibrate the

ligament parameters.

CHAPTER THREE: DEVELOPMENT OF A MODEL DATABASE OF HIGH BMI

SUBJECTS FOR EVALUATION OF IMPLANT DESIGN

Background

Obesity rates worldwide nearly tripled between 1975 and 2016, leading to some to refer to the issue as the 'obesity epidemic.' The World Health Organization defines obesity as an individual having a BMI greater than or equal to 30 kg/m^2 ("Obesity and overweight," 2021). In 2017, the Center for Disease Control and Prevention found that 42.4% of United States citizens suffered from obesity and 9.2% were severely obese (**Figure 10**) ("Adult Obesity Facts," 2021). A high BMI has been linked to negative health outcomes, including diabetes, hypertension, and a shorter life expectancy (Olshansky et al., 2005). Multiple studies have indicated that obesity is an independent cause of knee osteoarthritis which is commonly treated with a joint replacement procedure (Felson et al., 1987; Manek et al., 2003; Oliveria et al., 1999). A 2016 study showed that obesity confers a 100% increase in the risk that an individual will have to undergo a TKA procedure (Leyland et al., 2016).
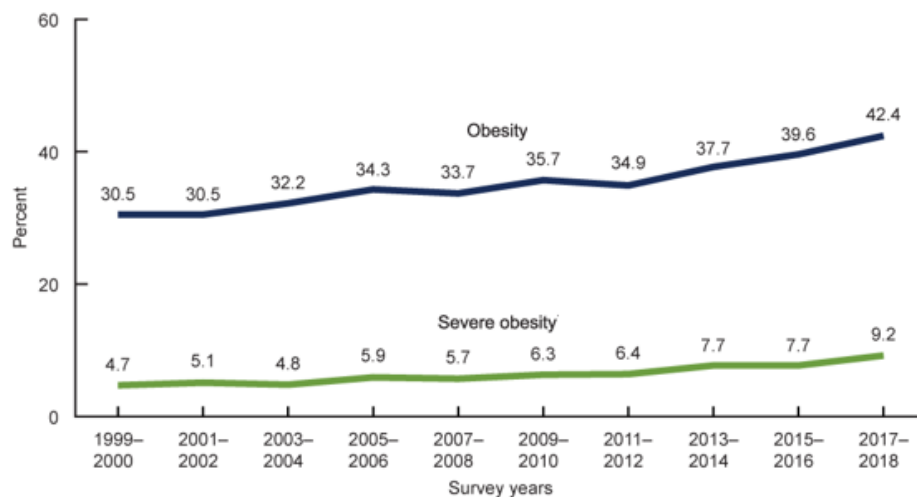
Figure 10. Obesity and severe obesity rates as a percentage of the total adult population from 1999 to 2018 ("Adult Obesity Facts," 2021).

The majority of published research on obesity's relation to TKA indicates that it is likely to have a negative impact on the procedure (Foran et al., 2004a, 2004b; Mulhall et al., 2010). Alignment of the limb following a TKA procedure plays an important role in the load distribution through the implant. The neutral position is defined as a less than 3° varus or valgus alignment of the mechanical axis of the limb (**Figure 11**). Following a TKA procedure, the repaired limb does not conform to this neutral alignment in obese individuals (Estes et al., 2013). Obese patients who undergo TKA have worse range of motion, lower Knee Society and Function scores (KSS – a measure of knee function based upon clinician input and patient experience), and longer operating times leading to increased rates of infection and complication following the procedure as compared to individuals with a normal BMI (Sun and Li, 2017). Obesity has been shown to result in worse surgical outcomes leading to increased revisions and reoperations (Wagner et al., 2016). However, even with the increase in negative outcomes, it has been shown that obese patients benefit from and should therefore not be refused the procedure (Yeung et

al., 2011). This holds true even for the morbidly obese (BMI $\geq$ 40 kg/m^2) who experience

better KSS ratings following a TKA procedure (Samson et al., 2010).

Figure 11. **Mechanical axis of the knee. A deviation of ± 3° is considered mal-aligned. Obesity has been linked to malalignment of this mechanical axis (Estes et al., 2013).**

Better understanding of obesity's impact on joint mechanics and kinematics at the

knee will allow for the development of prosthetics that are better suited to this

population. Computational models are crucial tools in predicting how knee replacement

devices will perform in vivo within the patient population (Martin et al., 2017; Pal et al.,

2008; Shu et al., 2020). However, prior investigations of TKA prosthetics have mostly

focused on a population with BMIs in the normal range, ignoring the growing portion of

the population that is at high risk of negative outcomes from the procedure. One study

found that from 2002 to 2009 obese individuals went from 6% of total TKAs performed

to 20% and a separate study found that the prevalence of obesity among TKA patients is

growing at 0.97% per year (George et al., 2017; Odum et al., 2013). As this portion of TKAs performed on obese individuals continues to grow, the demand for better devices will grow concurrently.

The objective of this study is to use the FE method to develop a model library of three high BMI subjects as they complete five activities of daily living. These models will be used in the optimization of longer-lasting prosthetics for this cohort. By varying different aspects of an implant's geometry, altering surgical techniques to achieve better alignment, or having patients receive bariatric surgery prior to a TKA, it may be possible to bring the kinematics and force distribution in an obese individual's implant more in line with someone from a non-obese cohort. Industry partners are currently doing such analyses with the models generated as part of this study.

Methods

The lower limb FE model detailed in Chapter 2 was modified and applied in the current study. In addition to the PI controller used for the F-E profile, two other PI controllers were used in the development of this model library. A PI controller was used to control the I-E angle at the knee by applying a torque about the S-I axis at the ankle and an additional controller adjusted the A-P translations of the TF joint by applying a torque about the ankle F-E axis. Tuning the three controllers was an iterative, manual procedure that consisted of plotting target profiles that were generated from the experimentally measured HSSR data and the resulting profile from the parameters and then minimizing the RMSE between the two plots.

The ligament parameters were also tuned using a manual procedure. The parameters were adjusted to attempt to bring the actual profile in line with the target

profile for the first 0.1 seconds of the seated knee flexion simulation. This activity was used as there is no weight borne by the leg and the TF joint goes through a large range of motion which should recruit every ligament at some point during the trial. For this procedure, the only active controller was the F-E controller. The controller is slowly turned on during the first 0.25 seconds of the simulation to prevent it ramping muscle forces too quickly, causing instability in the simulation. Therefore, during the first part of the simulation, the main determining factors for the kinematics are the ligament forces and articular geometry. By adjusting ligaments slack lengths or linear stiffness values, it is possible to bring the target and actual values in alignment for the three DOFs of interest, F-E, I-E, and A-P. To adjust A-P positioning, the ACL and PCL parameters were adjusted. The I-E rotations are mainly determined by ligaments on the lateral and medial sides of the knee, predominantly the MCL and LCL, but also the PFL and ALS play a role. F-E rotations are largely controlled by muscle forces; however, the ACL and PCL can have a small influence on the alignment of this DOF. After the ligaments were calibrated, the other two PI controllers were turned on and the parameters of the PI control system were tuned.

The meshing software developed and released by Rodriguez-Vila et al contained scripts to allow for the generation of hexahedral meshes of tibial cartilage, femoral cartilage, and the menisci. However, the full lower limb model utilized in these studies contained patellar geometry and therefore, this meshing piece needed to be added into the scripts. The custom ray-tracing algorithm for the tibial cartilage was replicated and applied to the patellar geometry (**Figure 12**). Additionally, the original software created six rows of elements that varied in thickness through the depth of the cartilage. This is

useful if the goal of the study is to analyze how stress is propagated through the cartilage. In the current study, the goal was to understand overall forces and contact mechanics for the patients in the model base. Consequently, this number of elements through the cartilage serves to increase computation time without adding benefit for the objective. The software was altered to change to four equally sized elements spaced throughout the thickness of the cartilage.
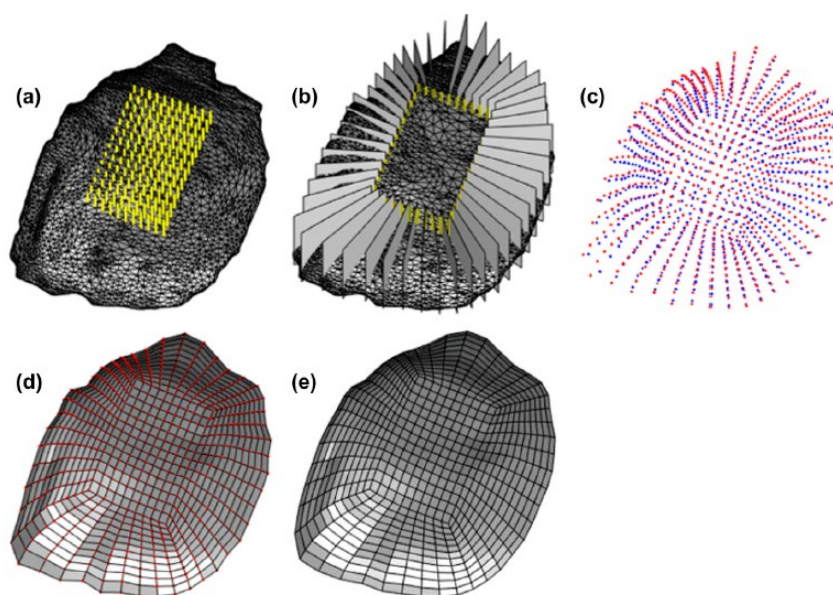
Figure 12.   Graphic showing the ray-tracing procedure developed for the tibial cartilage to go from an STL (a) to an optimized and smoothed hexahedral mesh (e). The procedure used here was replicated and reapplied to the patellar cartilage (Rodriguez-Vila et al., 2017).

For each of the five activities, the hip and ankle motions measured from the motion-capture system were kinematically prescribed in the model while the control system attempted to match the motions of the three DOF targets (F-E, I-E, and A-P) at the TF joint. The remaining three DOF (V-V, M-L, and S-I) were all left free to settle into a natural locus determined by contact between the femur and tibia articulating surfaces. Additionally, the PF joint was kinematically unconstrained in all DOF, with the

motion determined by the articulating geometry and forces from the patellar and quadriceps tendons. The medial and lateral PF ligaments maintained contact between the patellar and femoral cartilage.

Two of the three subjects in this analysis were simulated in the flexion, lunge, 90° pivot, chair rise, and step down activities. The third subject did not perform the chair rise activity and thus only four activities were included here. There were three versions of the simulation produced for each activity. The first version had the F-E PI controller turned on and tuned while the I-E and A-P DOF were left unconstrained to see how well the simulated joint would track in these two DOF. In version two, the I-E and A-P controllers were turned on and tuned. Finally, the third version extracted the I-E and A-P forces from the second version and applied directly without the use of the controller in these DOF.

Results

The 14 ligament bundles each had two properties that were tuned in the manual process, the linear stiffness and slack lengths. Iteration was required in order to achieve physiological forces for the ligament bundles. The manual tuning resulted in vastly different ligament properties between these three high BMI participants (**Table 5**). For instance, the ACLpl slack length varied from 22.5mm for one subject, but was found to be 35.0mm for a different subject. The large intersubject variability is one of the reasons that manual tuning is difficult. The slack lengths were found to be more variable than were the linear stiffness values. In all three subjects, the A-P profile was the most difficult to achieve a good match in the first 0.25s with the HSSR target data. Forces in the ACL or PCL along with the articular geometry were driving the limb into a different locus than was indicated by the HSSR data.

Table 5. **Resulting ligament properties for all three from the manual tuning.**

Bundle	Sub01		Sub02		Sub03	
	Slack Length (mm)	Linear Stiffness (N/mm)	Slack Length (mm)	Linear Stiffness (N/mm)	Slack Length (mm)	Linear Stiffness (N/mm)
ALS	26.39	20	26.39	20	26.39	20
ACLpl	29.11	240	22.53	240	35.03	165
ACLam	35.86	100	31.53	100	41.03	100
LCL	45.98	163	47.98	163	42.48	190
MCLa	58.54	75	56.54	75	54.54	85
MCLm	50.85	75	48.85	75	48.85	85
MCLp	46.84	75	44.84	75	47.34	85
dMCL	32.53	25	29.66	25	32.66	50
POL	33.48	35	33.48	35	32.48	50
PCAPl	43.80	110	43.80	110	40.80	110
PCAPm	42.27	100	42.27	100	40.27	100
PCLal	26.63	60	34.99	70	23.49	150
PCLpm	27.57	50	34.74	50	26.24	85
PFL	33.46	35	35.46	35	33.46	35

Tuning the PI controllers was also an iterative process that consisted of adjusting the gain factors for both the proportional and integral terms for each controller, leading to six gain values that needed to be tuned for each different activity the subjects were simulated performing. Largely, the PI controllers were tuned successfully in that the resulting kinematics matched the target profile well and did not result in large oscillations which are a common issue with PI controllers. A-P was always the most difficult DOF to match. An antagonistic relationship exists between the F-E and A-P controllers where an improvement in the A-P profile results in a worse match to the F-E profile and vice versa (**Figure 13**). The balance tended to require that the A-P profile tuning was not as accurate as the other two DOF. The gain values were scaling the applied muscle forces for the quadriceps and hamstrings in the case of the F-E PI controller and the ankle torques for the A-P and I-E controllers. These muscle forces were divided between the individual point-to-point muscles in the simulation (e.g. the semimembranosus, biceps femoris long head, and biceps femoris short head in the case of the hamstrings).
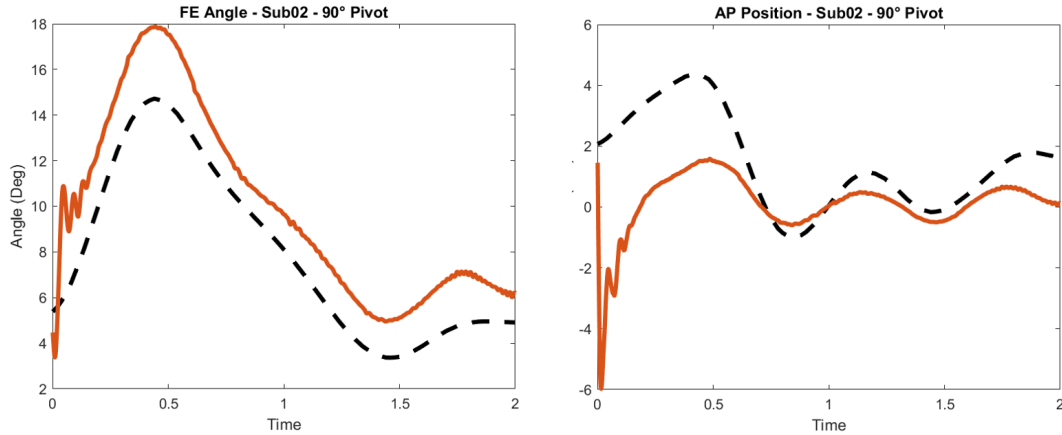
Figure 13. **F-E angle and A-P position plots for Sub02 in the 90° Pivot activity. HSSR target profile (black) and results from the PI tuning (red) plotted. As the F-E profile gets closer to the target in the last 0.25s, the A-P profile equivalently worsens.**

The muscle forces varied between the three subjects in this study with different activities resulting in the largest muscle forces. For two subjects, the lunge activity required the largest quadriceps force. The third subject had a large quadriceps force in this activity, but for that subject, the largest force was seen in the chair rise activity. For all three subjects, the largest hamstring force was seen in the seated flexion activity which is consistent with expectations given the unweighted nature of that activity and the range of motion the limb was undergoing. Maximum compressive pressure also varied between subjects and activities. The 90° pivot activity had the largest femoral and patellar cartilage pressure for Sub01 while the maximum tibial pressure was seen in the lunge activity. Step down produced the maximum femoral pressure for Sub02 (**Figure 14**), while pivot had the highest patellar pressure and chair rise had the max tibial pressure. Sub03 saw the maximum femoral and patellar pressures in the lunge activity and the maximum tibial pressure in the flexion activity.
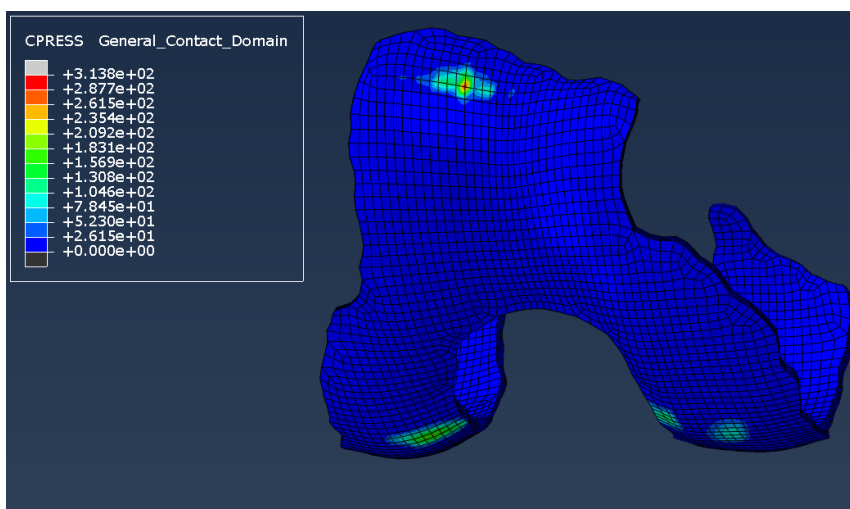
Figure 14.   Contact pressure plot for Sub02 femoral cartilage in the step down activity.

Discussion

The method utilized in the development of these models can be applied to many different datasets. In fact, the models developed in this study are part of a larger group of 12 subject datasets that were collected to compare the effects of increasing BMI on knee prosthetics. Ultimately, the model database will comprise the six high BMI and six normal BMI subjects whose data were used in the ligament sensitivity study. By creating simulations of high and normal BMI subjects in normal daily activities, researchers have a means of comparing kinematics in a natural and implanted knee. The models developed will be virtually implanted with a prosthetic device and the implanted knee will be simulated in the same activities that have already been simulated. Comparisons of the resulting kinematics will guide implant developers on potential changes that can be made to these devices to better accommodate this patient population. As well as changes to the implant design, different surgical techniques can also be evaluated, for example to evaluate optimal implant alignment for an obese individual. The end result of these simulations will be the development of cohort-specific designs for high BMI patients.

These experiments are not possible in vivo due to ethical considerations, but can be quantitatively evaluated and compared in these simulations.

Comparing between the three subjects in this study did not result in a clear trend regarding peak muscle forces or maximum compressive forces. The ligament tuning resulted in very different properties for these three subjects. Adding additional subjects to the model library has the potential to differentiate between the high and normal BMI populations. The benefit of this current analysis is not only in the results presented here, but from the fact that these models will be used in the creation of better prosthetic devices for a segment of the population that has been largely overlooked in current prosthetic development.

There are some limitations that exist in this model database that can be improved in future revisions. Due to the current setup of the F-E PI controller, only one muscle group is active at a given time. If the target profile has more flexion than is occurring in the model, the control system will turn up the hamstring forces to achieve this and essentially turn off the quadriceps with only a small force being applied to restrain the patella. This is not physiological as it is understood that in a certain range of motion, there is coactivation of the hamstrings and quadriceps. Future versions of these simulations should be created in order to allow for coactivation of these muscle bodies. Additionally, more refinement of the soft tissues of the TF joint, potentially in the form of membrane elements for ligaments and three-dimensional muscle models, would allow for a better representation of the natural knee that is being modelled.

CHAPTER FOUR: CONCLUSION

Summary

The primary goal of this research was to develop a means of using dynamic, in vivo kinematics to determine a range of physiological ligament properties for use in FE simulations. The software developed was used to create bounding areas for both high and normal BMI subjects. These bounding areas were compared between these two cohorts, as well as compared for age and gender differences. The largest effect size seen in the study was found with the ACLpl bundle between the high and normal BMI groups. The ACL and majority of the MCL were found to differ between high and normal BMI groups. To the author's knowledge, no prior study has focused on looking at differences between knee ligaments in these populations. Ligament laxity and the relationship with age and gender were also explored with gender being found to influence the properties of ligaments more so than age. Gender differences were found for ligaments that were on the medial and lateral sides of the knee (ALS, LCL, MCLa, MCLm, MCLp, and PFL) whereas age differences were found in internal, medial, and lateral ligaments (ACLam, ACLpl, MCLa, and PFL).

A secondary goal was the creation of a model database for use in simulating obese individuals in multiple activities of daily living. This database will be used for the simulation of the same obese and non-obese individuals with virtual implantation of a prosthetic device. The comparison of the natural, non-implanted knee will allow for assessment of an implant's viability in the obese population. Given the reports in

literature regarding failure in this cohort, it is likely that new prosthetic devices or surgical techniques are needed to allow for better implant survivability (Foran et al., 2004a, 2004b; Mulhall et al., 2010). The successful replication of the experimental kinematics in these simulations is a valuable first step to achieving the goal of a comprehensive database for testing a prosthetic's application in high BMI individuals.

Limitations

Due to the computational nature of these studies, simplifications were made that need to be addressed. The kinematics used in both of the objectives have uncertainty due to issues with the data collection and then translation into Abaqus. The retroreflective markers used are not solidly connected to the subject and therefore can move independent from the subject's bone that they are made to represent causing issues in the hip and pelvic motions. This is alleviated at the TF joint by the use of the HSSR data, but even the HSSR data is not perfect, hence the recalculation procedure used in pursuit of the sensitivity analysis. The model used for recalculation was simple, and therefore, is not a perfect recreation of the subject's motions.

Additionally, the subject-specific geometry created from the MRI and CT scans has errors from the manual nature used in extracting the bones and soft tissues from these scans. Some of the finer details are lost in translating these scans into 3D models of the TF joint. Smoothing applied at multiple levels loses some of the cartilage tissue from the final 3D model. The ligaments and muscles used were approximated as simple point-to-point connectors for computational efficiency and other soft tissues were left out of the model entirely for the same reason. Menisci, skin, and adipose tissue were removed from the final geometry used. The adipose tissue in particular could play a significant role in

the knee mechanics, particularly in the high BMI subjects. Research has already been done to quantify the impact that thigh-calf contact plays in the force distribution in the TF joint, and this was not accounted for in the present study (Zelle et al., 2009). As well as geometric simplifications, the material properties used for the simulations were simplifications on the realistic properties that would be found in TF tissues. Assuming linear pressure-overclosure relationships is beneficial from a computation time perspective, but ignores the complex interactions that may influence the resulting kinematics. Even with the simplifications and assumptions built into the process, the models created are still useful and will be used for the evaluation of prosthetic devices.

Future Work

The process and software developed for the ligament sensitivity analysis has aspects that could be improved in subsequent analyses. Firstly, the failure criteria should be reevaluated. The rupture forces of the ligament were deemed to be excessive for a study focused on finding physiological ligament properties leading to the 80% of rupture force that was used, but given the lack of other restraining tissues in the knee, there is an argument for allowing the ligaments to carry additional force. Alternatively, the model could be enhanced by the inclusion of some of these tissues while retaining the same ligament maximum force capacity. The 25N minimum force requirement was also arbitrarily chosen and should be reconsidered in future implementations of this procedure.

Subsequent models built from the three high BMI subject's simulations could be more complex through additions of some of the tissues previously mentioned. There also exists refinements that could be made to the PI controllers, such as adding the

coactivation of the quadriceps and hamstrings. Adding in additional activities from the HSSR data that was already collected would serve to allow for better validation of the prosthetics being tested with this dataset. Lastly, adding all 12 subjects into this database is currently a work in progress and will greatly improve the likelihood that successful new devices can be built that will alleviate the issues that currently exist in current implants.

REFERENCES

Adult Obesity Facts [WWW Document], 2021. . Cent. Dis. Control Prev. URL
www.cdc.gov/obesity/data/adult.html

Aggelis, D.G., Paschos, N.K., Barkoula, N.M., Paipetis, A.S., Matikas, T.E., Georgoulis,
A.D., 2011. Rupture of anterior cruciate ligament monitored by acoustic emission.
J. Acoust. Soc. Am. 129, EL217–EL222. https://doi.org/10.1121/1.3571537

Blankevoort, L., Huiskes, R., de Lange, A., 1991. Recruitment of Knee Joint Ligaments.
J. Biomech. Eng. 113, 94–103. https://doi.org/10.1115/1.2894090

Butler, D.L., Guan, Y., Kay, M.D., Cummings, J.F., Feder, S.M., Levy, M.S., 1992.
Location-dependent variations in the material properties of the anterior cruciate
ligament. J. Biomech. 25, 511–518. https://doi.org/10.1016/0021-9290(92)90091-
E

Chandrashekar, N., Mansouri, H., Slauterbeck, J., Hashemi, J., 2006. Sex-based
differences in the tensile properties of the human anterior cruciate ligament. J.
Biomech. 39, 2943–2950. https://doi.org/10.1016/j.jbiomech.2005.10.031

Ciccone, W.J., Bratton, D.R., Weinstein, D.M., Walden, D.L., Elias, J.J., 2006. Structural
Properties of Lateral Collateral Ligament Reconstruction at the Fibular Head. Am.
J. Sports Med. 34, 24–28. https://doi.org/10.1177/0363546505278704

Delp, S.L., Anderson, F.C., Arnold, A.S., Loan, P., Habib, A., John, C.T., Guendelman,
E., Thelen, D.G., 2007. OpenSim: Open-Source Software to Create and Analyze
Dynamic Simulations of Movement. IEEE Trans. Biomed. Eng. 54, 1940–1950.
https://doi.org/10.1109/TBME.2007.901024

Elias, J.J., Cosgarea, A.J., 2007. Computational Modeling: An Alternative Approach for
Investigating Patellofemoral Mechanics. Sports Med. Arthrosc. 15, 89–94.
https://doi.org/10.1097/JSA.0b013e31804bbe4d

Estes, C.S., Schmidt, K.J., McLemore, R., Spangehl, M.J., Clarke, H.D., 2013. Effect of Body Mass Index on Limb Alignment After Total Knee Arthroplasty. J. Arthroplasty 28, 101–105. https://doi.org/10.1016/j.arth.2013.02.038

Felson, D.T., Naimark, A., Anderson, J., Kazis, L., Castelli, W., Meenan, R.F., 1987. The prevalence of knee osteoarthritis in the elderly. the framingham osteoarthritis study. Arthritis Rheum. 30, 914–918. https://doi.org/10.1002/art.1780300811

Fitzpatrick, C.K., Clary, C.W., Rullkoetter, P.J., 2012. The role of patient, surgical, and implant design variation in total knee replacement performance. J. Biomech. 45, 2092–2102. https://doi.org/10.1016/j.jbiomech.2012.05.035

Foran, J.R.H., Mont, M.A., Etienne, G., Jones, L.C., Hungerford, D.S., 2004a. The outcome of total knee arthroplasty in obese patients. J. Bone Jt. Surg. - Ser. A 86, 1609–1615. https://doi.org/10.2106/00004623-200408000-00002

Foran, J.R.H., Mont, M.A., Rajadhyaksha, A.D., Jones, L.C., Etienne, G., Hungerford, D.S., 2004b. Total knee arthroplasty in obese patients: A comparison with a matched control group. J. Arthroplasty 19, 817–824. https://doi.org/10.1016/j.arth.2004.03.017

Galbusera, F., Freutel, M., Dürselen, L., D'Aiuto, M., Croce, D., Villa, T., Sansone, V., Innocenti, B., 2014. Material Models and Properties in the Finite Element Analysis of Knee Ligaments: A Literature Review. Front. Bioeng. Biotechnol. 2. https://doi.org/10.3389/fbioe.2014.00054

George, J., Klika, A.K., Navale, S.M., Newman, J.M., Barsoum, W.K., Higuera, C.A., 2017. Obesity Epidemic: Is Its Impact on Total Joint Arthroplasty Underestimated? An Analysis of National Trends. Clin. Orthop. Relat. Res. 475, 1798–1806. https://doi.org/10.1007/s11999-016-5222-4

Grood, E.S., Suntay, W.J., 1983. A Joint Coordinate System for the Clinical Description of Three-Dimensional Motions: Application to the Knee. J. Biomech. Eng. 105, 136–144. https://doi.org/10.1115/1.3138397

Halloran, J.P., Petrella, A.J., Rullkoetter, P.J., 2005. Explicit finite element modeling of total knee replacement mechanics. J. Biomech. 38, 323–331. https://doi.org/10.1016/j.jbiomech.2004.02.046

Harner, C.D., Xerogeanes, J.W., Livesay, G.A., Carlin, G.J., Smith, B.A., Kusayama, T., Kashiwaguchi, S., Woo, S.L.-Y., 1995. The Human Posterior Cruciate Ligament Complex: An Interdisciplinary Study. Am. J. Sports Med. 23, 736–745. https://doi.org/10.1177/036354659502300617

Harris, M.D., Cyr, A.J., Ali, A.A., Fitzpatrick, C.K., Rullkoetter, P.J., Maletsky, L.P., Shelburne, K.B., 2016. A Combined Experimental and Computational Approach to Subject-Specific Analysis of Knee Joint Laxity. J. Biomech. Eng. 138. https://doi.org/10.1115/1.4033882

Hohenberger, G.M., Maier, M., Schwarz, A.M., Grechenig, P., Weiglein, A.H., Hauer, G., Leithner, A., Sadoghi, P., 2019. Correlation Analysis of the Anterolateral Ligament Length with the Anterior Cruciate Ligament Length and Patient's Height: An Anatomical Study. Sci. Rep. 9, 9802. https://doi.org/10.1038/s41598-019-46351-0

Hume, D.R., Kefala, V., Harris, M.D., Shelburne, K.B., 2018. Comparison of Marker-Based and Stereo Radiography Knee Kinematics in Activities of Daily Living. Ann. Biomed. Eng. 46, 1806–1815. https://doi.org/10.1007/s10439-018-2068-9

Ivester, J.C., Cyr, A.J., Harris, M.D., Kulis, M.J., Rullkoetter, P.J., Shelburne, K.B., 2015. A Reconfigurable High-Speed Stereo-Radiography System for Sub-Millimeter Measurement of In Vivo Joint Kinematics. J. Med. Device. 9. https://doi.org/10.1115/1.4030778

Kennedy, J.C., Hawkins, R.J., Willis, R.B., Danylchuck, K.D., 1976. Tension studies of human knee ligaments. Yield point, ultimate failure, and disruption of the cruciate and tibial collateral ligaments. J. Bone Joint Surg. Am. 58, 350–5.

LaPrade, R.F., Bollom, T.S., Wentorf, F.A., Wills, N.J., Meister, K., 2005. Mechanical Properties of the Posterolateral Structures of the Knee. Am. J. Sports Med. 33, 1386–1391. https://doi.org/10.1177/0363546504274143

Leyland, K.M., Judge, A., Javaid, M.K., Diez-Perez, A., Carr, A., Cooper, C., Arden, N.K., Prieto-Alhambra, D., 2016. Obesity and the Relative Risk of Knee Replacement Surgery in Patients With Knee Osteoarthritis: A Prospective Cohort Study. Arthritis Rheumatol. 68, 817–825. https://doi.org/10.1002/art.39486

Manek, N.J., Hart, D., Spector, T.D., MacGregor, A.J., 2003. The association of body mass index and osteoarthritis of the knee joint: An examination of genetic and environmental influences. Arthritis Rheum. 48, 1024–1029. https://doi.org/10.1002/art.10884

Martin, J.R., Jennings, J.M., Watters, T.S., Levy, D.L., McNabb, D.C., Dennis, D.A., 2017. Femoral Implant Design Modification Decreases the Incidence of Patellar Crepitus in Total Knee Arthroplasty. J. Arthroplasty 32, 1310–1313. https://doi.org/10.1016/J.ARTH.2016.11.025

Mulhall, K., Ghomrawi, H., Mihalko, W., Cui, Q., Saleh, K., 2010. Adverse Effects of Increased Body Mass Index and Weight on Survivorship of Total Knee Arthroplasty and Subsequent Outcomes of Revision TKA. J. Knee Surg. 20, 199–204. https://doi.org/10.1055/s-0030-1248043

Naghibi Beidokhti, H., Janssen, D., van de Groes, S., Hazrati, J., Van den Boogaard, T., Verdonschot, N., 2017. The influence of ligament modelling strategies on the predictive capability of finite element models of the human knee joint. J. Biomech. 65, 1–11. https://doi.org/10.1016/j.jbiomech.2017.08.030

O'Brien, S., Luo, Y., Wu, C., Petrak, M., Bohm, E., Brandt, J.M., 2013. Computational development of a polyethylene wear model for the articular and backside surfaces in modular total knee replacements. Tribol. Int. 59, 284–291. https://doi.org/10.1016/J.TRIBOINT.2012.03.020

Obesity and overweight [WWW Document], 2021. . World Heal. Organ. https://doi.org/10.1016/j.med.2020.07.010

Odum, S.M., Springer, B.D., Dennos, A.C., Fehring, T.K., 2013. National Obesity Trends in Total Knee Arthroplasty. J. Arthroplasty 28, 148–151. https://doi.org/10.1016/J.ARTH.2013.02.036

Oliveria, S.A., Felson, D.T., Cirillo, P.A., Reed, J.I., Walker, A.M., 1999. Body weight, body mass index, and incident symptomatic osteoarthritis of the hand, hip, and knee. Epidemiology 10, 161–6.

Olshansky, S.J., Passaro, D.J., Hershow, R.C., Layden, J., Carnes, B.A., Brody, J., Hayflick, L., Butler, R.N., Allison, D.B., Ludwig, D.S., 2005. A Potential Decline in Life Expectancy in the United States in the 21st Century. N. Engl. J. Med. 352, 1138–1145. https://doi.org/10.1056/NEJMsr043743

Pal, S., Haider, H., Laz, P.J., Knight, L.A., Rullkoetter, P.J., 2008. Probabilistic computational modeling of total knee replacement wear. Wear 264, 701–707. https://doi.org/10.1016/j.wear.2007.06.010

Peters, A.E., Akhtar, R., Comerford, E.J., Bates, K.T., 2018. Tissue material properties and computational modelling of the human tibiofemoral joint: a critical review. PeerJ 6, e4298. https://doi.org/10.7717/peerj.4298

Race, A., Amis, A.A., 1994. The mechanical properties of the two bundles of the human posterior cruciate ligament. J. Biomech. 27, 13–24. https://doi.org/10.1016/0021-9290(94)90028-0

Rachmat, H.H., Janssen, D., Verkerke, G.J., Diercks, R.L., Verdonschot, N., 2015. Material properties of the human posterior knee capsule. Biomed. Mater. Eng. 25, 177–187. https://doi.org/10.3233/BME-151268

Rahnemai-Azar, A.A., Miller, R.M., Guenther, D., Fu, F.H., Lesniak, B.P., Musahl, V., Debski, R.E., 2016. Structural Properties of the Anterolateral Capsule and Iliotibial Band of the Knee. Am. J. Sports Med. 44, 892–897. https://doi.org/10.1177/0363546515623500

Robinson, J.R., Bull, A.M., Amis, A.A., 2005. Structural properties of the medial collateral ligament complex of the human knee. J. Biomech. 38, 1067–1074. https://doi.org/10.1016/j.jbiomech.2004.05.034

Rodriguez-Vila, B., Sánchez-González, P., Oropesa, I., Gomez, E.J., Pierce, D.M., 2017. Automated hexahedral meshing of knee cartilage structures – application to data from the osteoarthritis initiative. Comput. Methods Biomech. Biomed. Engin. 20, 1543–1553. https://doi.org/10.1080/10255842.2017.1383984

Saha, S., Roychowdhury, A., 2009. Application of the Finite Element Method in Orthopedic Implant Design. J. Long. Term. Eff. Med. Implants 19, 55–82. https://doi.org/10.1615/JLongTermEffMedImplants.v19.i1.70

Samson, A.J., Mercer, G.E., Campbell, D.G., 2010. Total knee replacement in the morbidly obese: a literature review. ANZ J. Surg. 80, 595–599. https://doi.org/10.1111/j.1445-2197.2010.05396.x

Shin, C.S., Chaudhari, A.M., Andriacchi, T.P., 2007. The influence of deceleration forces on ACL strain during single-leg landing: A simulation study. J. Biomech. 40, 1145–1152. https://doi.org/10.1016/j.jbiomech.2006.05.004

Shu, L., Li, S., Sugita, N., 2020. Systematic review of computational modelling for biomechanics analysis of total knee replacement. Biosurface and Biotribology 6, 3–11. https://doi.org/10.1049/bsbt.2019.0012

Sun, K., Li, H., 2017. Body mass index as a predictor of outcome in total knee replace: A systemic review and meta-analysis. Knee 24, 917–924. https://doi.org/10.1016/j.knee.2017.05.022

Wagner, E.R., Kamath, A.F., Fruth, K., Harmsen, W.S., Berry, D.J., 2016. Effect of Body Mass Index on Reoperation and Complications After Total Knee Arthroplasty. J. Bone Jt. Surg. 98, 2052–2060. https://doi.org/10.2106/JBJS.16.00093

Weiss, J.A., Gardiner, J.C., Ellis, B.J., Lujan, T.J., Phatak, N.S., 2005. Three-dimensional finite element modeling of ligaments: Technical aspects. Med. Eng. Phys. 27, 845–861. https://doi.org/10.1016/j.medengphy.2005.05.006

Woo, S.L.-Y., Hollis, J.M., Adams, D.J., Lyon, R.M., Takai, S., 1991. Tensile properties of the human femur-anterior cruciate ligament-tibia complex. Am. J. Sports Med. 19, 217–225. https://doi.org/10.1177/036354659101900303

Yeung, E., Jackson, M., Sexton, S., Walter, W., Zicat, B., Walter, W., 2011. The effect of obesity on the outcome of hip and knee arthroplasty. Int. Orthop. 35, 929–934. https://doi.org/10.1007/s00264-010-1051-3

Zelle, J., Barink, M., De Waal Malefijt, M., Verdonschot, N., 2009. Thigh–calf contact: Does it affect the loading of the knee in the high-flexion range? J. Biomech. 42, 587–593. https://doi.org/10.1016/J.JBIOMECH.2008.12.015